

Fabrication of carbon nanotube hybrid films as transparent electrodes for small-molecule photovoltaic cells.

Y. Zhou,^{a,*} Z Wang,^b T. Saito,^c T. Miyadera,^b M. Chikamatsu,^b S. Shimada,^a R. Azumi^a

a. Electronics and Photonics Research Institute, National Institute of Advanced Industrial Science and Technology (AIST), 1-1-1 Higashi, 305-8565, Tsukuba, Japan

b. Research Center for Photovoltaics, National Institute of Advanced Industrial Science and Technology (AIST), 1-1-1 Higashi, 305-8565, Tsukuba, Japan

c. Nanomaterials Research Institute, National Institute of Advanced Industrial Science and Technology (AIST), 1-1-1 Higashi, 305-8565, Tsukuba, Japan

*E-mail: y-shuu@aist.go.jp

Electronic Supplementary Information

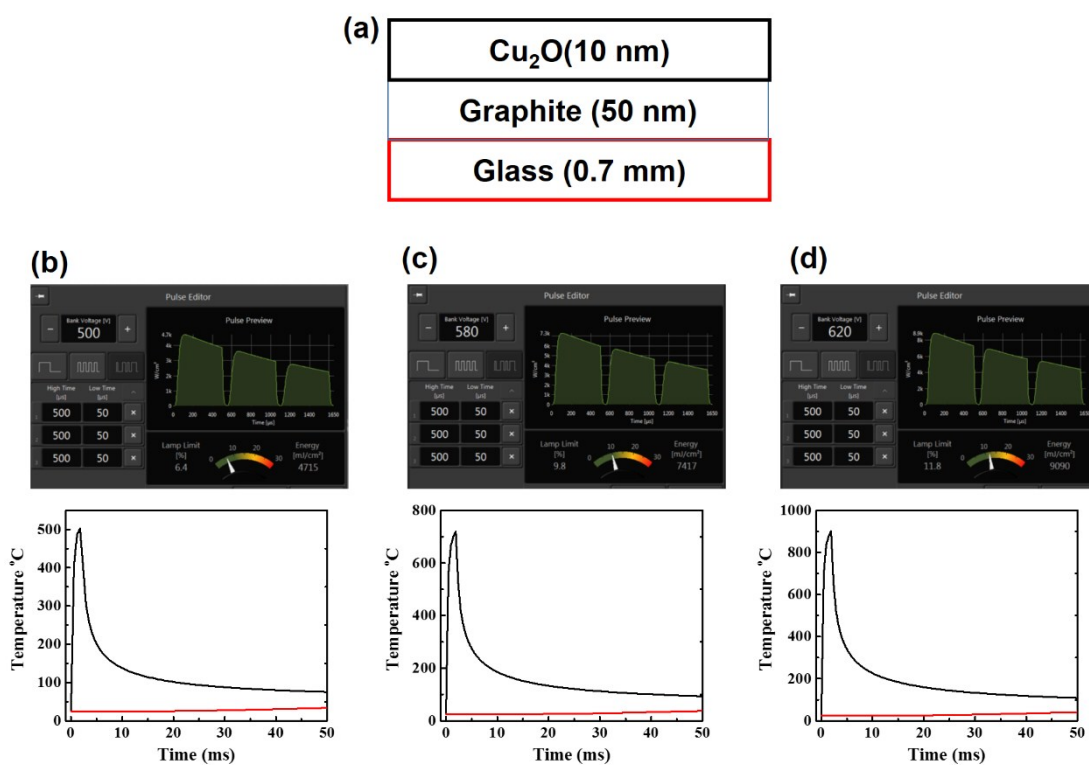


Fig.S1 The details in the photonic curing process: (a) structural models with graphite and copper oxide as replacements of carbon nanotube and copper iodide, and (b) (c) (d) three typical process parameters and corresponding simulated thermal processes. The voltage and pulse are used to efficiently control the photonic power. In spite of the

fact that the simulation is too rough to monitor the exact process, we can clearly see the rapid heating and cooling process. Especially, the peak temperature drops within 0.001 second for each shot. This method also enables the high temperature process at a low substrate temperature. In the present work, (b) was used to remove dispersant, and (c) and (d) were used to construct CNT-CuI and CNT-MoO₃ hybrid films, respectively. The curing processes can be repeated many times to control the degree of doping.

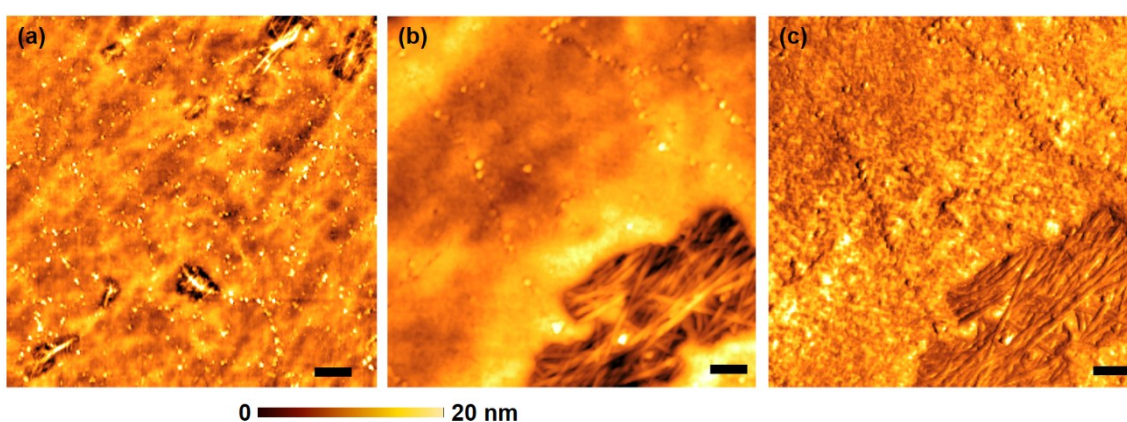


Fig. S2 (a) Large scale and (b) small scale AFM images of the CNT/CuI film before photonic curing. (c) AFM phase image of (b). The scale bars are 500 and 100 nm for (a) and (b), respectively. These images are taken by scanning at different area in the same sample shown in Fig. 1(c). Apparently, because of the large surface roughness and hydrophobic properties of CNT networks, the spin-coated CuI film did not fully cover the surface of CNT. It shows that CuI forms a continuous film with a thickness of about 10 nm, while CuI did not permeate into the porous CNT networks.

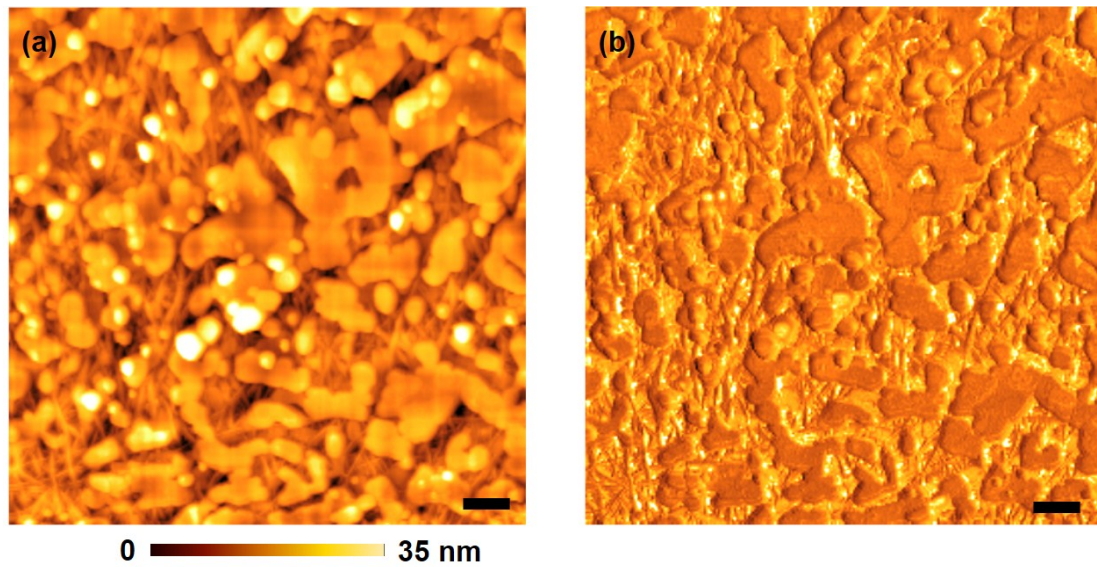


Fig. S3 AFM (a) height and (b) phase images of the CNT-Cul films after 10 times photonic curing with process parameters shown in Fig. S1(c). The scale bars are 200 nm. We note that the continuous Cul film shown in Fig. S2 is divided into several smaller agglomerates and nanoparticles. It indicates that photonic curing causes the structural evolution of CNT-Cul film. CNT-Cul hybrid film shown in Fig. 1(d) is finally formed after another 20-30 times of photonic curing shorts, resulting in the smallest sheet resistance. Similar method is used for CNT-MoO₃, and whose structural evolution is shown in Fig. 3.

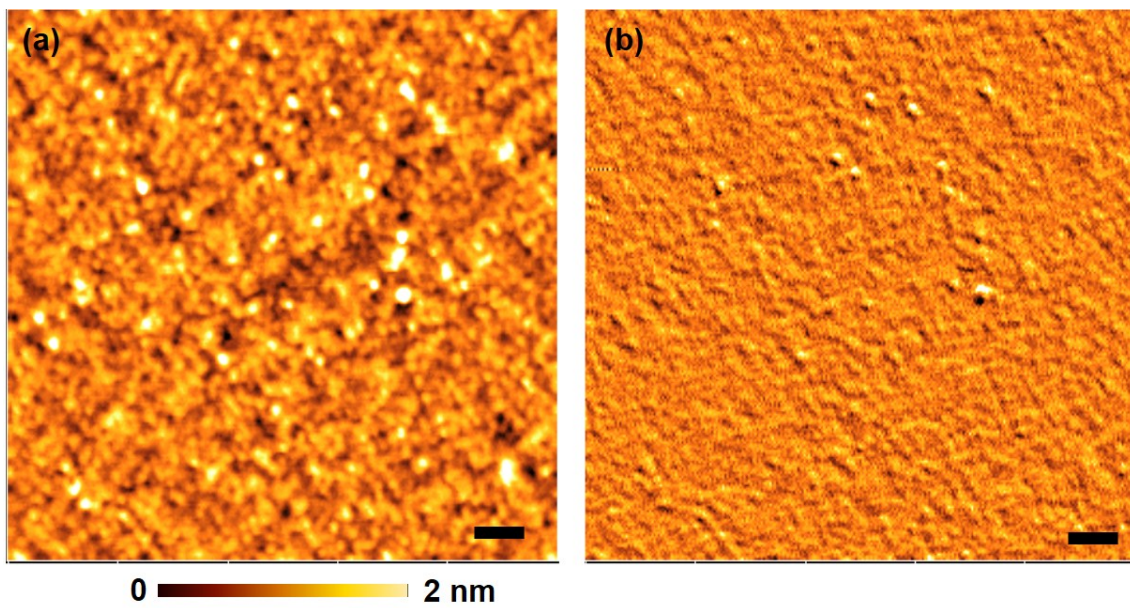


Fig. S4 AFM (a) height and (b) phase images of the 10 nm-thick MoO_3 film on glass substrate. The scale bars are 100 nm. Evaporated MoO_3 exhibits nanoparticles with grain sizes of around 10 nm. These MoO_3 nanoparticles cannot be observed in the CNT network in Fig. 3(a).